piRNAs mediate posttranscriptional retroelement silencing and localization to pi-bodies in the *Drosophila* germline

Ai Khim Lim,[1,2] Liheng Tao,[1] and Toshie Kai[1,2]

[1]Temasek Life Sciences Laboratory and [2]Department of Biological Sciences, The National University of Singapore, 117604 Singapore

Nuage, a well-conserved perinuclear organelle found in germline cells, is thought to mediate retroelement repression in *Drosophila melanogaster* by regulating the production of Piwi-interacting RNAs (piRNAs). In this study, we present evidence that the nuage–piRNA pathway components can be found in cytoplasmic foci that also contain retroelement transcripts, antisense piRNAs, and proteins involved in messenger RNA (mRNA) degradation. These mRNA degradation proteins, decapping protein 1/2 (DCP1/2), Me31B (maternal expression at 31B), and pacman (PCM), are normally thought of as components of processing bodies. In *spindle-E* (*spn-E*) and *aubergine* (*aub*) mutants that lack piRNA production, piRNA pathway proteins no longer overlap the mRNA degradation proteins. Concomitantly, *spn-E* and *aub* mutant ovaries show an accumulation of full-length retroelement transcripts and prolonged stabilization of *HeT-A* mRNA, supporting the role of piRNAs in mediating posttranscriptional retroelement silencing. *HeT-A* mRNA is derepressed in mRNA degradation mutants *twin*, *dcp1*, and *ski3*, indicating that these enzymes also aid in removing full-length transcripts and/or decay intermediates.

Introduction

The fidelity of genomic information in the germline has to be tightly regulated for accurate transmission to the next generation. In many animal germline cells, Piwi-interacting RNAs (piRNAs) are reported to silence the expression of one class of mobile genetic elements, retroelements, whose transposition may afflict the genome with mutational burden (Lau et al., 2006; Vagin et al., 2006; Aravin et al., 2007; Houwing et al., 2007). In flies and mammals, the Piwi subfamily proteins are engaged in a feed-forward loop to mediate the generation of sense and antisense piRNAs from the active transposons and piRNA clusters (Vagin et al., 2006; Aravin et al., 2007; Brennecke et al., 2007; Houwing et al., 2007). This amplification cycle could contribute to the removal of both strands of retroelement transcripts via a processing mechanism. However, sense piRNAs are present at very low levels in wild-type ovaries (Vagin et al., 2006), and antisense retroelement transcripts are not as abundant as their sense counterparts when processing is compromised in the male and female germlines (Aravin et al., 2001; Savitsky et al., 2006; Chambeyron et al., 2008; Shpiz et al., 2009). This suggests distinct silencing mechanisms other than the feed-forward processing loop, which could remove the sense strand transcripts. Possible mechanisms include piRNA-mediated transcriptional/cotranscriptional silencing via chromatin modifications and posttranscriptional destabilization of retroelement transcripts.

Cellular mRNA turnover is mediated by conventional mRNA degradation enzymes, such as the decapping enzymes, deadenylases, and exoribonucleases. Some of these enzymes and RNA-binding proteins, such as GW182, are reported to localize to the processing bodies, the putative site where mRNAs are degraded (for review see Anderson, 2005; Eulalio et al., 2007; Parker and Sheth, 2007). Biochemical analyses have demonstrated that the processing body components GW182 and DCP1 interact with the RNA-induced silencing complexes (RISCs) argonaute 1 (AGO1) and AGO2 in mammalian cells (Liu et al., 2005a,b; Behm-Ansmant et al., 2006) and that the *Caenorhabditis elegans* homologue of GW182, AIN-1, interacts with a putative AGO family protein ALG-1 (Ding et al., 2005). In addition, RISCs have been reported to localize to the

Correspondence to Toshie Kai: toshie@tll.org.sg

Abbreviations used in this paper: CDS, coding sequence; DIG, digoxygenin; LM, ligation mediated; MCP, MS2 coat protein; PAT, poly(A) tail test; piRNA, Piwi-interacting RNA; RACE, rapid amplification of cDNA ends; RISC, RNA-induced silencing complex; rRNA, ribosomal RNA; UTR, untranslated region.

The Rockefeller University Press $30.00
J. Cell Biol. Vol. 186 No. 3 333–342
www.jcb.org/cgi/doi/10.1083/jcb.200904063

processing bodies in human cultured cells (Liu et al., 2005b; Sen and Blau, 2005; Jagannath and Wood, 2009), implying that small RNA-mediated mRNA degradation and/or translational repression could take place in the processing bodies.

Several lines of evidence have implicated the involvement of the nuage, a well-conserved structure in animal germline cells, in posttranscriptional silencing. In *Drosophila melanogaster*, Dicer-1 and AGO2 are mislocalized in a nuage component mutant *maelstrom*, suggesting a connection between the nuage and microRNA pathway (Findley et al., 2003). Consistent with this, processing body proteins DCP1a and GW182 and microRNAs let-7 and miR-21 are reported to colocalize with the mouse nuage (Kotaja et al., 2006; Beaudoin et al., 2009). In the *suppressor of stellate*–deficient testes aubergine (*aub*), spliced *stellate* transcript accumulates, and stellate protein is dramatically translated (Kotelnikov et al., 2009), implying that stellate expression is regulated posttranscriptionally. In *C. elegans*, processing body components PATR-1, CCF-1, DCAP2, and CGH-1 have been demonstrated to overlap with P granules (a counterpart of the nuage) in the germline blastomeres (Lall et al., 2005; Gallo et al., 2008). Besides, the presence of abundant processing bodies in *Drosophila* germline cells (Lin et al., 2008) implies that posttranscriptional regulation is actively taking place and may therefore aid in retroelement decay.

In this study, we show that the piRNA pathway proteins, retroelement transcripts, piRNAs, and mRNA degradation components localize to common cytoplasmic foci. We demonstrate that *HeT-A* mRNA is stabilized in the piRNA pathway mutant *aub* and derepressed in the mRNA degradation mutants *twin*, *dcp1*, and *ski3*. These findings suggest that posttranscriptional retroelement silencing is piRNA dependent and that some mRNA degradation enzymes assist in removing the retroelement transcripts. Localization of the piRNA and mRNA degradation components into common foci may reflect the assembly of a macromolecular complex dedicated to the removal of retroelement transcripts.

Results and discussion

Two Piwi subfamily proteins, aubergine (AUB) and AGO3, and a tudor domain protein, KRIMP, have been described previously to localize in perinuclear foci called the nuage in *Drosophila* germline cells (Snee and Macdonald, 2004; Brennecke et al., 2007; Lim and Kai, 2007). Interestingly, we observed that these nuage components also existed in cytoplasmic foci that were 0.1–1 µm in diameter (Fig. 1 a, arrows; Harris and Macdonald, 2001). These cytoplasmic foci became progressively prominent from stage 4 onwards during oogenesis and were ubiquitously distributed as discrete puncta throughout the nurse cell cytoplasm at stages 4–5 (Fig. 1 a). The spatial and temporal distributions of these cytoplasmic foci resemble the processing bodies described in the *Drosophila* germline (Lin et al., 2008). We costained for the processing body components dDCP1, dDCP2 (Lin et al., 2006), Me31B (a homologue of yeast-decapping activator Dhh1p; Coller et al., 2001), and the *Drosophila* homologue of yeast Xrn1p, pacman (PCM; Till et al., 1998; Barbee et al., 2006; Zabolotskaya et al., 2008). 40–57%, 38–51%, and 31–79% of the processing bodies were found to overlap or dock AUB, AGO3, and KRIMP foci, respectively (Fig. 1, b [arrows], c, and d). This large percentage variation suggests that the association of cytoplasmic nuage with processing bodies is highly dynamic. We also observed processing body foci that lacked the piRNA pathway components (Fig. 1, b and e, arrowheads), suggesting that a subset of processing bodies contains piRNA pathway components, whereas others do not. These observations imply that cytoplasmic foci identifiable as the processing bodies include molecular complexes with distinct functions, as reflected by their different compositions.

Nuage components are reported to mediate retroelement repression in the germline (Lim and Kai, 2007; Pane et al., 2007). To ask whether the cytoplasmic foci containing the nuage and processing body components are involved in retroelement silencing, we looked for the presence of the retroelement transcripts using the MS2 coat protein (MCP)–GFP-labeling system (Forrest and Gavis, 2003). We generated flies harboring two heat shock–inducible transgenes. One contained *HeT-A* or *I-element* coding sequences (CDSs), devoid of the 5′ untranslated region (UTR) and promoter regions, and fused to six tandem stem-loop–binding sites for bacteriophage MCP at the 3′ UTR. The other encoded for the fusion protein MCP-GFP. Upon induction, MCP-GFP binds the recognition motif on *HeT-A–(ms2)$_6$* or *I-element–(ms2)$_6$* transcripts so that these mRNAs can be visualized as GFP signal.

In control (*aub* or *krimp* heterozygote) ovaries, GFP signal was found in cytoplasmic foci that were also stained for the 5′ to 3′ exoribonuclease PCM and the piRNA pathway protein KRIMP (Fig. 2, a and a', arrows). These GFP-labeled foci were not detected in the ovary expressing MCP-GFP alone (Fig. 2 a), indicating that GFP signals represent full-length *HeT-A–(ms2)$_6$* transcripts or the decay intermediates harboring MCP-binding sites. Similarly, we observed the localization of GFP-labeled *I-element* transcript to KRIMP/PCM foci in the wild-type ovary (Fig. 2 a, arrows). Using a nonretroelement control *nanos* (*nos*), we did not observe localization of *nos-(ms2)$_6$* to distinct cytoplasmic bodies (Fig. 2 a″; Forrest and Gavis, 2003), confirming that the localization of the retroelement transcripts is not artifactual. In *aub* and *krimp* mutant ovaries, the GFP-labeled *HeT-A* transcript no longer localized to the cytoplasmic KRIMP foci (Fig. 2 a). Instead, it appeared to be diffuse in the cytoplasm and nucleus, indicating that the granular localization of the transcripts observed in the control ovaries depends on AUB and KRIMP functions.

AUB and AGO3 complexes are reported to associate with piRNAs in the germline (Gunawardane et al., 2007; Nishida et al., 2007). In addition, recombinant AUB and AGO3 are competent for cleaving a substrate RNA at an siRNA target site (Gunawardane et al., 2007), indicating that these AGO proteins are potential constituents of germline RISCs. To determine whether the nuage cytoplasmic foci consist of piRNA-loaded germline RISCs, we examined the localization of antisense piRNAs by FISH. The antisense *HeT-A* piRNA signals colocalized with the GFP–*HeT-A* foci in the *aub* control ovary (Fig. 2, b and b′, arrows), whereas an irrelevant probe hybridizing to antisense 2S ribosomal RNA (rRNA) or a piRNA-unrelated

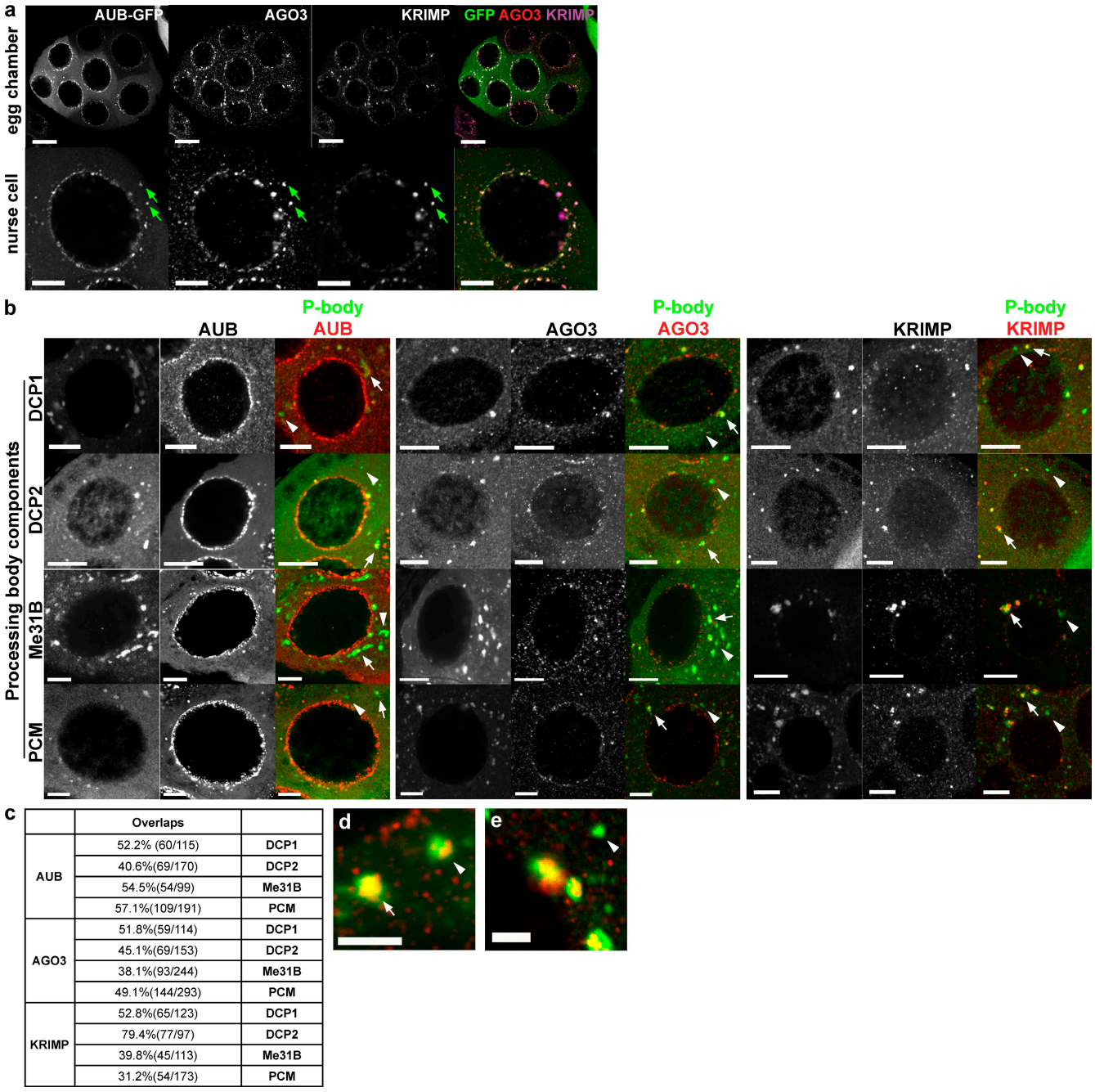

	Overlaps	
AUB	52.2% (60/115)	DCP1
	40.6%(69/170)	DCP2
	54.5%(54/99)	Me31B
	57.1%(109/191)	PCM
AGO3	51.8%(59/114)	DCP1
	45.1%(69/153)	DCP2
	38.1%(93/244)	Me31B
	49.1%(144/293)	PCM
KRIMP	52.8%(65/123)	DCP1
	79.4%(77/97)	DCP2
	39.8%(45/113)	Me31B
	31.2%(54/173)	PCM

Figure 1. **Nuage cytoplasmic foci overlap with mRNA degradation proteins in germline cells.** (a) Nuage–piRNA pathway components exhibit both perinuclear and cytoplasmic foci. AUB-GFP (green), AGO3 (red), and KRIMP (magenta) cytoplasmic foci colocalize (arrows) in stage 4–5 egg chamber. Bars: (top) 20 µm; (bottom) 10 µm. (b) Nuage cytoplasmic foci overlap mRNA degradation proteins of the processing bodies (P bodies). AUB, AGO3, and KRIMP cytoplasmic bodies (red) overlap with mRNA degradation proteins dDCP1, dDCP2, Me31B, and PCM (green; arrows). A subset of P body foci does not overlap with nuage cytoplasmic foci (arrowheads). All images represent a single confocal section. Bars, 10 µm. (c) Overlaps of cytoplasmic nuage and P body foci. Overlaps that are quantified in d include complete overlaps and partial overlaps that consist of nuage cytoplasmic foci docking partially around the mRNA degradation components. Overlapping nuage–P body foci are expressed as percentages of the total number of overlapping and nonoverlapping P body foci. The range of overlaps (complete or partial) appears to be independent of the foci sizes and nuage–P body pairs. (d) Immunostaining of overlapping cytoplasmic AGO3 (red) and Me31B (green) foci. A complete overlap and partial overlap are indicated by an arrow and an arrowhead, respectively. Bar, 4 µm. (e) Immunostaining of nonoverlapping Me31B. An Me31B focus (green) that lacks the cytoplasmic KRIMP (red) and is indicated by an arrowhead. Bar, 4 µm.

HeT-A antisense region did not exhibit any significant colocalization (Fig. 2, b and b"; and not depicted). A control staining with secondary antibodies alone did not exhibit nonspecific labeling of the GFP–*HeT-A* foci (unpublished data), further indicating the specificity of *HeT-A* piRNA probe. In *aub* mutants in which the production of piRNAs is impaired (Vagin et al., 2006), the antisense *HeT-A* piRNA signal was undetectable (Fig. 2 b). Similarly, we observed specific antisense *HeT-A* piRNA signal in control but not *krimp* mutant ovaries (unpublished data). The localization of both piRNAs and the target

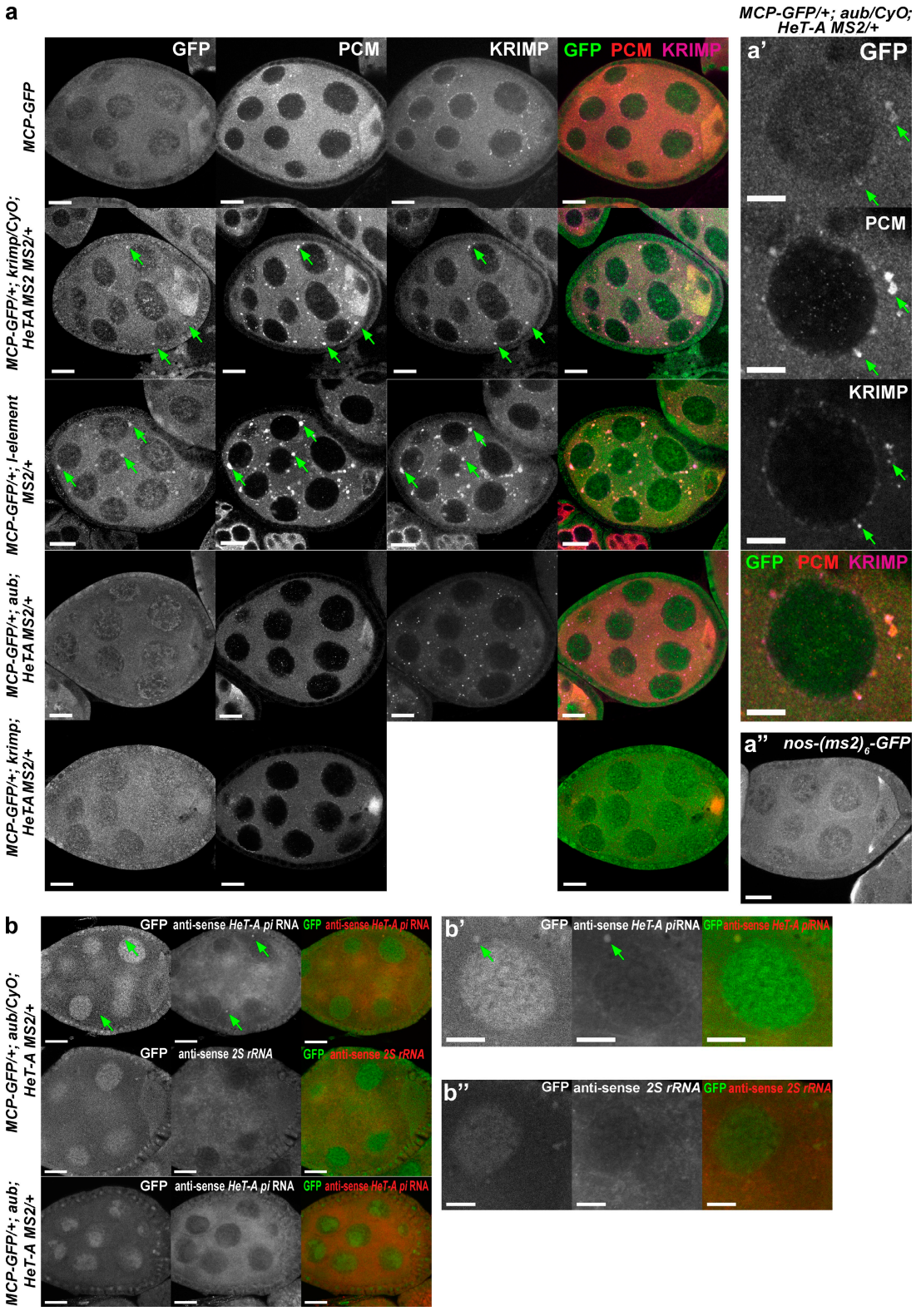

Figure 2. **Retroelement transcripts and antisense piRNAs colocalize with nuage cytoplasmic foci and mRNA degradation proteins (pi-bodies).** (a and a′) Immunostaining of ovaries expressing MCP-GFP fusion protein and the transgene of retroelements harboring MCP-binding sites (*HeT-A*–$[ms2]_6$ or *I-element*–$[ms2]_6$) in control (*aub* or *krimp* heterozygotes) and *aub* or *krimp* mutants. *HeT-A*–$(ms2)_6$ or *I-element*–$(ms2)_6$ tagged with GFP colocalizes with the piRNA pathway component KRIMP (magenta) and 5′→3′ exoribonuclease PCM (red) in the same cytoplasmic foci (a′, arrows). In *aub* and *krimp* mutants, GFP-labeled *HeT-A* mRNA appears to be largely cytoplasmic and nuclear and no longer localizes to the cytoplasmic KRIMP foci. (a″) A nonretroelement control *nos(ms2)*$_6$ recapitulates the endogenous mRNA localization at the oocyte posterior, but no localization to distinct cytoplasmic bodies is observed. Bars: (egg chambers) 20 µm; (nurse cells) 10 µm. (b) FISH for antisense *HeT-A* piRNAs in *aub* mutant. (b′) In the *aub* control ovary, antisense *HeT-A* piRNAs colocalize with GFP-labeled *HeT-A* mRNA in the same cytoplasmic bodies (arrows). FISH with the control probe against antisense 2S rRNA does not colocalize with GFP-labeled *HeT-A* mRNA. In *aub* mutant, unique antisense *HeT-A* piRNA signal is undetectable. Bars, 10 µm.

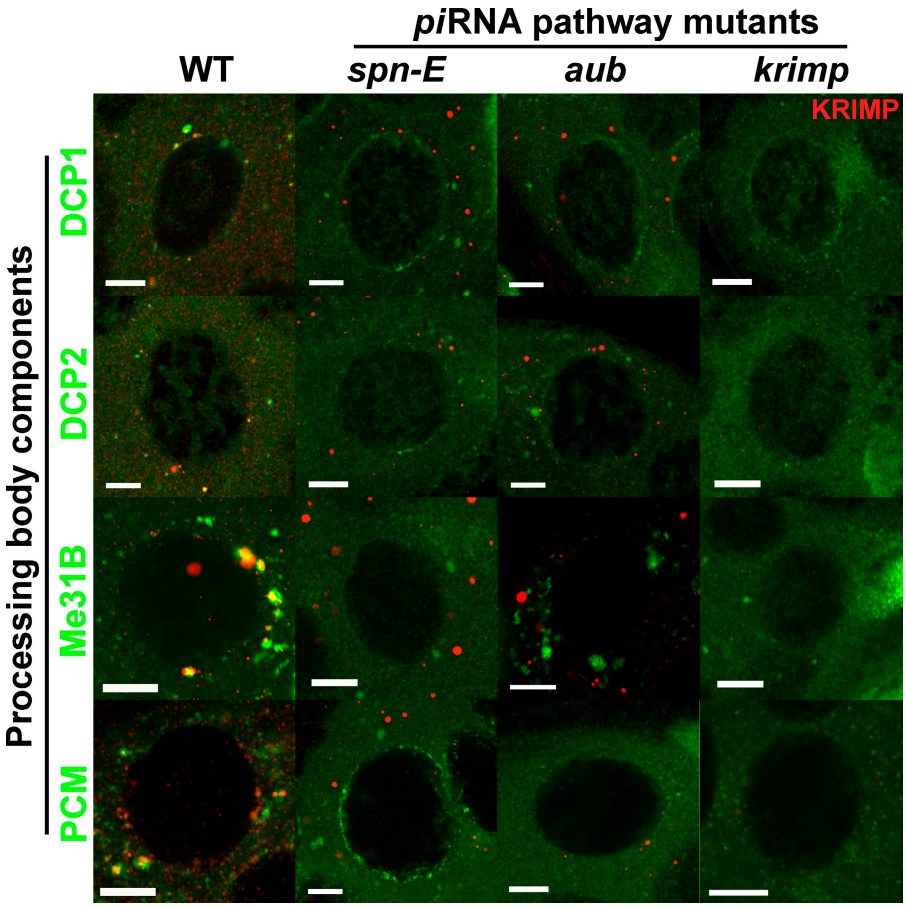

Figure 3. **Assembly of the pi-bodies is piRNA dependent.** In the wild-type (WT) ovaries, the mRNA degradation proteins dDCP1/2, Me31B, and PCM overlap cytoplasmic KRIMP foci. In contrast, in piRNA pathway mutants *spn-E* and *aub* in which the production of piRNAs is compromised, cytoplasmic KRIMP foci no longer overlap with the mRNA degradation proteins. Bars, 10 µm.

transcripts to common foci that possibly contain the mRNA degradation proteins reflect the assembly of a macroRNP complex committed to the removal of retroelement transcripts. To distinguish them from conventional processing bodies, we termed these foci pi-bodies.

In *spindle-E* (*spn-E*) and *aub* mutants in which the production of piRNAs is compromised (Vagin et al., 2006; Chen et al., 2007), we did not detect any cytoplasmic KRIMP foci that overlap with dDCP1/2, Me31B, and PCM (Fig. 2 a and Fig. 3), indicating that pi-body assembly is disrupted. This observation suggests that cytoplasmic nuage proteins and the targeted mRNAs are recruited to mRNA degradation components, or vice versa, in a piRNA-dependent manner, forming pi-bodies that can contribute to retroelement silencing.

To exclude the possibility that the failure of pi-body assembly in s*pn-E* and *aub* mutants impairs the activities of mRNA degradation proteins and results in retroelement silencing, we checked two representative activities of mRNA turnover: deadenylation and decapping of a nonretroelement transcript *cyclin B* (*cycB*). The rapid degradation of the *cyclin* transcripts has been shown to be regulated by deadenylation (Morris et al., 2005). To monitor deadenylation activity, we examined the length of the *cycB* poly(A) tail in the *aub* mutant using the poly(A) tail test (PAT; Fig. 4 a; Salles et al., 1999). In comparison with the deadenylase mutant *twin* in which deadenylation was compromised and longer poly(A) tails were observed, *cycB* transcript appeared to be efficiently deadenylated in the *aub* mutant. This indicates that deadenylation is unaffected in the piRNA pathway mutants.

To examine decapping, total RNAs extracted from both control and *aub* mutant ovaries were treated with Terminator 5′-phosphate–dependent exonuclease and subjected to RT-PCR for *cycB*. RNA molecules with 5′ cap structures are protected from the exonuclease and therefore competent for amplification. Similar to the control, *cycB* transcript was comparably degraded by the exonuclease in the *aub* mutant (Fig. 4 b), indicating that *cycB* mRNA is efficiently decapped. Furthermore, we did not detect any changes in the protein expression of four mRNA degradation proteins: PCM, SKI3, Me31B, and dDCP1 in *aub* or *krimp* mutants (Fig. 4 c). Collectively, these data show that the retroelement-silencing defect in the piRNA pathway mutants is not caused by impairment of the mRNA degradation machinery.

To determine whether piRNA-mediated retroelement silencing is posttranscriptional in vivo, we investigated retroelement decay in the *aub* control and mutant ovaries using the inducible *HeT-A* transgene harboring MS2. After the induction of *HeT-A* MS2 mRNA by heat shock, ovaries were dissected at time intervals up to 12 h, and Northern blotting was performed with a probe that specifically detects exogenous *HeT-A* MS2. In the control ovary, *HeT-A* MS2 mRNA was rapidly degraded, and the level of transcript was undetectable by 100 min after induction (Fig. 5 a). However, in the *aub* mutant, *HeT-A* mRNA exhibited prolonged stabilization (Fig. 5, a and a') and remained detectable 2–3 d after induction (not depicted). This suggests

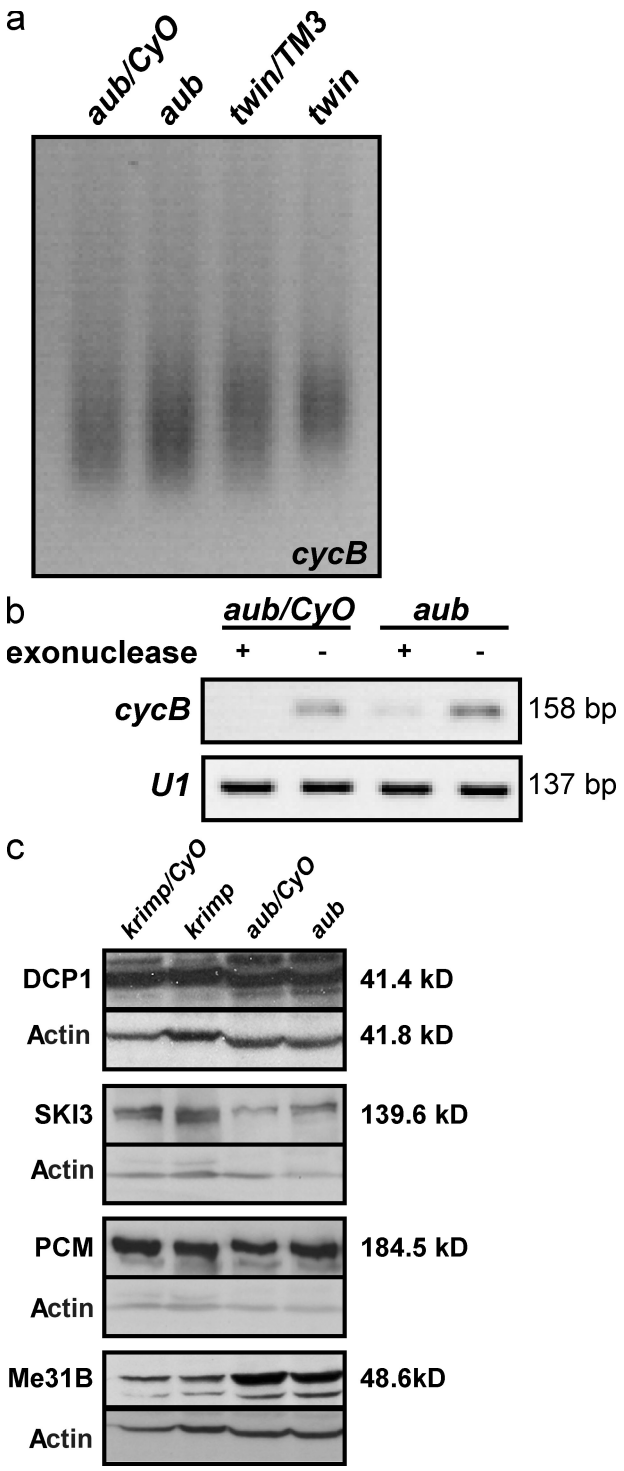

Figure 4. **mRNA degradation activities and protein expression are unaffected in piRNA pathway mutants.** (a) LM-PAT assay of *cycB*. In the piRNA pathway mutant *aub*, deadenylation appears unaffected because the poly(A) tail length is comparable with that of the control. In contrast, deadenylation is impaired in the deadenylase mutant *twin*, as indicated by the accumulation of longer poly(A) tails. (b) Cap analysis of *cycB*. In *aub* mutants as well as in the control, the 5′ UTR of *cycB* is efficiently degraded by Terminator 5′-phosphate–dependent exonuclease, indicating that decapping of *cycB* takes place normally. The control small nuclear RNA *U1*, which harbors a 2,2,7-trimethyl G cap, is resistant to exonuclease treatment. (c) Western analyses of mRNA degradation protein expression in the piRNA pathway mutants. Expression of DCP1, SKI3 (a component of 3′→5′ SKI–exosome), PCM, and Me31B is unaffected in *aub* and *krimp* mutants.

that a prolonged posttranscriptional retroelement silencing is dependent on piRNAs.

spn-E mutation causes down-regulation of the repressive chromatin marks H3K9me2 and H3K9me3 at the retroelement promoters, implying that piRNA-dependent retroelement expression is regulated at the transcriptional level (Klenov et al., 2007). Our data further indicate that piRNA-mediated retroelement silencing is in part posttranscriptional. Collectively, at least two hierarchies of retroelement surveillance appear to function in the fly germline: posttranscriptional regulation in the cytoplasm and transcriptional control in the nucleus. Because our exogenous *HeT-A* transcript was under the control of an inducible promoter and was efficiently repressed in the control ovary, the contribution of natural promoters or UTRs in mediating silencing is ruled out. This also emphasizes posttranscriptional retroelement silencing by piRNAs in trans. However, it remains possible that piRNAs are targeted to the nascent transcript and silence *HeT-A* cotranscriptionally.

We observed significant accumulations of endogenous full-length *HeT-A* and *I-element* transcripts in *spn-E*, *aub*, and *krimp* mutants (Fig. 5 b). Furthermore, a low level of full-length *HeT-A* transcript accumulated in the deadenylase mutant *twin*, indicating the involvement of the mRNA degradation enzymes in the posttranscriptional silencing of retroelements either in a piRNA-dependent or -independent manner. We did not observe either of the full-length retroelements or decay intermediates in *dcp1*, *ski3*, or *pcm* mutants (Fig. 5 b and Fig. S1). However, a more sensitive quantitative assay, rapid amplification of cDNA ends (RACE)–PAT/RT-PCR, detected derepression of the CDS, UTRs, and poly(A) regions of *HeT-A* mRNA in *dcp1* and *ski3* mutants (Fig. 5 c), further indicating that removal of the retroelement transcripts and/or the decay intermediates involves mRNA degradation enzymes.

We did not detect an obvious reduction of *HeT-A* and *I-element* antisense piRNAs in *twin*, *dcp1*, *ski3*, and *pcm* mutants as compared with the respective control heterozygotes (Fig. S2 a). Furthermore, we observed normal perinuclear and cytoplasmic localization of proteins involved in piRNA production, AUB, AGO3, and KRIMP in the mRNA degradation mutants (Fig. S2 b). These observations suggest that piRNA biogenesis is unaffected and does not contribute to retroelement derepression in those mutants.

Foregoing work has suggested the nuage as a potential site for RISC-mediated posttranscriptional retroelement silencing (Harris and Macdonald, 2001; Kennerdell et al., 2002; Findley et al., 2003; Brennecke et al., 2007; Li et al., 2009; Malone et al., 2009). The 5′ and 3′ moieties of the decay intermediates generated by RISC-mediated endoribonucleolytic cleavage are removed by the XRN1–exosome and SKI–exosome complexes, respectively, in S2 cells (Orban and Izaurralde, 2005). Using the *Drosophila* ovary as an in vivo system, we have reported the localization of the germline AGO proteins, AUB and AGO3, and mRNA degradation enzymes in the pi-bodies, implying that the mRNA degradation machinery mediates the posttranscriptional removal of the retroelement transcripts or decay intermediates, possibly upon piRNA-mediated cleavage. The absence of retroelement decay intermediates in vivo in our blotting analyses with single

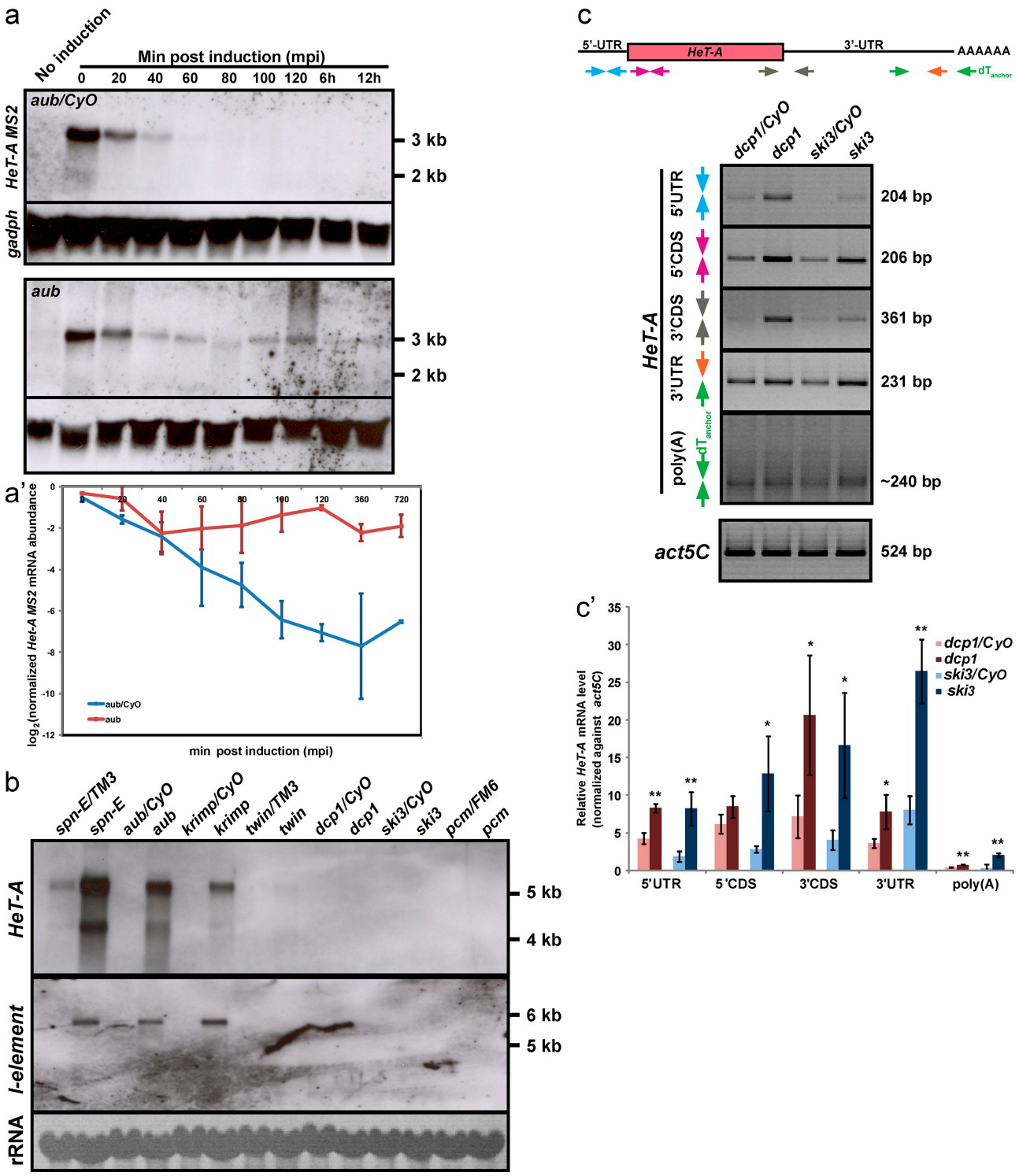

Figure 5. **Posttranscriptional retroelement silencing is piRNA dependent.** (a) Time course of *HeT-A* MS2 mRNA decay in the *aub* mutant. *HeT-A* MS2 expression is induced by heat shock, and changes in mRNA abundance are measured over time. A rapid initial degradation of *HeT-A* MS2 mRNA is observed in both control and *aub* mutant ovaries. However, *aub* mutant exhibits prolonged stabilization of the *HeT-A* MS2 transcript, whereas the exogenous mRNA is undetectable in control ovaries by 100 mpi. (a') Graphical output of normalized *HeT-A* MS2 transcript against *gadph* mRNA in control and *aub* mutant ovaries ($n = 3$). (b) Northern blotting of endogenous retroelement transcripts in the piRNA pathway and mRNA degradation mutants. Full-length *HeT-A* and *I-element* transcripts accumulate in *spn-E*, *aub*, and *krimp* mutants at steady state. A low level of full-length *HeT-A* mRNA accumulates in the deadenylase mutant *twin*. No detectable full-length retroelement transcript is observed in the mRNA degradation mutants *dcp1*, *ski3*, and *pcm*. (c) Semiquantitative RACE-PAT and RT-PCR analyses of retroelement expression in the mRNA degradation mutants. The schematic diagram shows primer sets (arrows) that are used to amplify regions on *HeT-A*, 5′ UTR, CDS, 3′ UTR, and poly(A). All examined regions are derepressed in *dcp1* and *ski3* mutants. (c') Quantitative RACE-PAT and RT-PCR of *HeT-A* mRNA normalized against *act5C* in *dcp1* and *ski3* mutants. Error bars indicate the standard deviation between the triplicates of each sample. *, $P < 0.05$; **, $P < 0.01$ ($n = 3$).

mRNA degradation mutants may reflect the redundancy of other enzymes mediating degradation. However, we cannot exclude the possibility that mRNA degradation genes contribute to posttranscriptional silencing of the retroelements via a piRNA-independent pathway. We have also provided evidence that retroelement silencing is regulated posttranscriptionally in a piRNA-dependent manner. This involves contributions from both the nuage and mRNA degradation proteins. In addition to AUB, AGO3, and KRIMP, we also observed the localization of other nuage components to the same cytoplasmic nuage bodies (unpublished data), suggesting that posttranscriptional retroelement silencing utilizes a large RNP complex or subcomplexes. Future understanding of the signaling pathways and players that regulate the assembly of *Drosophila* pi-bodies will shed new light on the development of host–parasite communities.

Materials and methods

Fly strains and transgenes

For ovary staining, *y w* was used as a wild-type control unless otherwise stated. Mutant alleles and allelic combinations used in this study were *aub*$^{HN2/N11}$ (Schupbach and Wieschaus, 1991; Wilson et al., 1996), *spn-E*$^{616/hls3987}$ (Gillespie and Berg, 1995; Gonzalez-Reyes et al., 1997), *b53; T3* (an insertion mutant for *dcp1* that harbors a rescue transgene for a neighboring gene, CG5602; Lin et al., 2006), *krimp*^{f06583} (Lim and Kai, 2007), *twin*^{KG00877}/Df(3R)crb-F89-4, *ski3*^{f03251}/Df(2R)Np5 (Bloomington *Drosophila* Stock Center), and *pcm*$^{\Delta 1}$ (Fig. S1). Me31B-GFP fly line was obtained from Carnegie Protein Trap Library (Buszczak et al., 2007). Flies carrying the transgene UASp-*aub-GFP* (Harris and Macdonald, 2001) or UASp-*dcp1*-HA (Lin et al., 2006) were crossed to flies harboring the nosgal4VP16 transgene to drive the expression of tagged proteins in the female germline (Van Doren et al., 1998).

Immunostaining

Ovaries were dissected, stained, and mounted as described previously in Lim and Kai (2007). The following antibodies were used: anti-KRIMP rabbit polyclonal (1:10,000; Lim and Kai, 2007), anti-KRIMP rat polyclonal (1:500), anti-AUB rabbit polyclonal (1:1,000; provided by H. Han, McGill University, Montreal, Quebec, Canada), anti-AGO3 mouse (1:500), anti-dDCP1 rabbit polyclonal (1:20; Lin et al., 2006), anti-dDPC2 rabbit polyclonal (1:200; Lin et al., 2006), anti-Me31B mouse monoclonal (1:500; provided by A. Nakamura, RIKEN Center for Developmental Biology, Kobe, Hyogo, Japan), anti-PCM rabbit polyclonal (1:500; Barbee et al., 2006), anti-HA mouse monoclonal (1:500; BEAM-ETC), and anti-GFP mouse monoclonal 3E6 (1:200; Invitrogen). Alexa Fluor (488, 555, or 633)–conjugated goat anti–mouse, anti–rat, and anti–rabbit secondary antibodies (1:400; Invitrogen) were used. Images were captured at room temperature with a 3-PMT detector using a 40 or 63× 1.3 NA Plan Apochromat oil objective in an upright confocal microscope (EXCITER or LSM510; Carl Zeiss, Inc.) controlled by LSM5 program software (Carl Zeiss, Inc.). For quantification of cytoplasmic nuage and P body overlaps in Fig. 1 c, single confocal sections of stages 5–7 egg chambers were counted manually. At least three egg chambers from different ovarioles were scored for each nuage–P body combination. For AUB, which exhibited fewer cytoplasmic foci, 5–8 egg chambers were scored.

Generation of antibodies

Krimp (amino acids 461–540), *ski3* (amino acids 1,131–1,233), and *ago3* (amino acids 78–252) antigen sequences were amplified with EST clones RE66405, LP07472, and LD17152, respectively. All primer sequences are provided in Table S1. Each fragment was cloned into pENTR/D-TOPO (Invitrogen) and recombined into pDEST$_{15}$ GST (Invitrogen) according to the manufacturer's instructions. GST fusion proteins were purified using glutathione Sepharose high performance (GE Healthcare) and used for antibody generation in mice for AGO3 and in rats for KRIMP and SKI3.

Generation and characterization of *pcm*$^{\Delta 1}$ and *ski3*^{f03251} mutant alleles

A P element insertion line, EP1526, was used to generate a *pcm* mutant allele using a standard excision protocol. One mutant allele, *pcm*$^{\Delta 1}$, was isolated by single-fly PCR using the primers *pcm*-Ex forward and *pcm*-Ex reverse (Table S1). For *ski3*, the piggyBac insertion line f03251 exhibited no apparent phenotype and was cleaned up by backcrossing to *y w*.

Western blotting

Ovary lysates were prepared as described previously in Drummond-Barbosa and Spradling (2004). Rabbit anti-PCM polyclonal, rat anti-SKI3 polyclonal, rabbit anti-dDCP1, mouse anti-Me31B, and mouse antiactin monoclonal JLA20 (Developmental Studies Hybridoma Bank) were used at 1:2,000, 1:500, 1:1,000, 1:2,500, and 1:1,500, respectively. Detection was performed using rabbit-, rat-, and mouse-conjugated HRP (1:6,000–1:10,000; Bio-Rad Laboratories).

MS2/MCP-GFP labeling of retroelement transcripts

HeT-A or *I-element* genomic sequences and six tandem stem-loop–binding sites for MCP were amplified using *y w* genomic DNA and pSL-MS2-6 (Bertrand et al., 1998) as templates, respectively. All primer sequences are provided in Table S1. Amplified *HeT-A* was digested with XbaI and BglII and cloned into pCaSpeR-hs. Amplified *I-element* was cloned into pGEM-T Easy, digested with NotI, and recloned into pCaSpeR-hs. pGEM-T Easy harboring six copies of MCP-binding sites was digested with EcoRI, blunted with Klenow fragment, and ligated into the StuI site of pCaSpeR-hs *HeT-A* and the blunted XbaI site of pCaSpeR-hs *I-element*, respectively. These plasmids were microinjected into *y w* embryos using standard methods. The transgenes, *HeT-A–(ms2)$_6$*, *I-element–(ms2)$_6$* or the control *nos-(ms2)$_6$*, and *MCP-GFP* (Forrest and Gavis, 2003) were coexpressed in *aub* or *krimp* control and mutants by subjecting female flies to a heat shock regimen of 1.5 h at 36°C every 12 h for a duration of 1.5 d. Immunostaining was performed 2 d after heat shock.

piRNA FISH

Digoxygenin (DIG)-labeled RNA probes were transcribed using double-stranded DNA harboring a T7 promoter and the antisense *HeT-A* piRNA or 2S rRNA sequence (Table S1). Fixed ovaries were washed in PBS containing 0.1% (wt/vol) Tween 20 and hybridized at 42°C overnight in Hyb buffer (0.5 µg/µl yeast tRNA, 50% dextran sulfate, 100 mM Pipes, pH 8.0, 10 mM EDTA, pH 8.0, and 3 M NaCl; Pontes et al., 2006) containing 2 µg denatured RNA probes. Ovaries were washed sequentially in 2× SSC/50% formamide, 1× SSC/50% formamide, and 1× SSC and PBS/0.1% (wt/vol) Triton X-100 for 10 min each. DIG-labeled RNA probes were detected using anti-DIG HRP antibody (1:100; Roche) with fluorescence amplification (tyramide signal amplification kit; PerkinElmer).

Time course of *HeT-A* MS2 mRNA decay

aub control and mutant flies harboring *HeT-A–(ms2)$_6$* were subjected to 2 h of heat shock at 36°C. Ovaries were dissected in cold Grace's medium at 0, 20, 40, 60, 80, 100, and 120 min and 6 and 12 h after heat shock termination and immediately frozen in TRIzol reagent (Invitrogen) at −80°C until RNA extraction. For mRNA abundance measurement, band intensities corresponding to *HeT-A* MS2 were quantified using ImageJ (National Institutes of Health) and normalized to *gadph* transcript.

Northern blotting

Total RNA was extracted from ovaries with TRIzol reagent according to the manufacturer's instructions. For analysis of *HeT-A* MS2 mRNA, DIG DNA probes were synthesized with T7 and SP6 primers using pGEM-T Easy MS2 as a template. For analysis of endogenous *HeT-A*, *I-element*, and *gadph* transcripts, DIG DNA probes were synthesized with High Prime DNA Labeling kit (Roche) using pCaSpeR-hs *HeT-A–(ms2)$_6$*, pCaSpeR-hs *I-element–(ms2)$_6$*, and amplified full-length *gadph* (Table S1) as templates, respectively. 5 µg total RNA was loaded and separated in a formaldehyde/MOPS 1% agarose gel, transferred onto a Hybond N+ nylon membrane (GE Healthcare), and cross-linked. Hybridization was performed at 45°C in DIG Easy Hyb buffer, and detection was performed according to the manufacturer's instructions (Roche). For stripping, the blots were incubated with boiling 0.5% SDS. rRNA was visualized using 0.02% (wt/vol) methylene blue.

For PAGE Northern analysis of piRNAs, RNA probes against *HeT-A* and *I-element* were synthesized from the linearized templates by in vitro transcription in the presence of DIG RNA-labeling mix (Roche; Lim and Kai, 2007). 10 µg total RNA from the ovaries was separated on a 15% polyacrylamide/8 M urea denaturing gel, transferred, and cross-linked as described for the agarose gel. Hybridization and detection were similarly performed with a temperature change to 62°C.

Ligation-mediated (LM) PAT assay

3 µg total RNA from ovaries was treated with DNaseI (Roche). LM-PAT assay was performed as described previously (Salles et al., 1999). Amplified

products were visualized on a 3% agarose/1× Tris Boric EDTA gel. All primer sequences can be found in Table S1.

Cap analysis

100 ng total RNA from ovaries was incubated with 1 U Terminator 5′-phosphate–dependent exonuclease (Epicentre) at 30°C for 3 h. Reactions were terminated by adding 0.5 µl 100 mM EDTA, pH 8.0. To check levels of *cycB* and *U1* expression, one-step RT-PCR was performed using diluted or neat total RNA according to the manufacturer's instructions (Invitrogen). All primer sequences can be found in Table S1.

RACE-PAT and RT-PCR

1–3 µg total RNA from ovaries was treated with DNaseI (Roche). Reverse transcription was performed using Oligo(dT)$_{anchor}$ and avian myeloblastosis virus reverse transcription (Promega) as described previously (Salles et al., 1999). A mock reaction without reverse transcription was prepared for each RNA sample. The newly synthesized cDNAs were checked for genomic DNA contamination by PCR with *actin5C* or *gadph* primers. PCR was subsequently performed using 1 µl diluted or neat cDNA sample/reaction. For analyses of retroelement derepression, primer sets corresponding to *actin5C* and *HeT-A* UTRs, CDS, and poly(A) regions were used. For the examination of mRNA expression in $pcm^{\Delta 1}$ and $ski3^{f03251}$ mutant alleles, primer sets corresponding to different regions of *pcm* or *ski3* and a neighboring gene of *pcm*, *nat1*, were used. All primer sequences can be found in Table S1.

The same cDNAs were used for quantitative PCR in the presence of iQ SYBR Green supermix (Bio-Rad Laboratories). For amplification and detection, a single-color real-time PCR detection system (MyQ; Bio-Rad Laboratories) was used. Control experiments measuring the change in C_T with template dilution demonstrated that the efficiencies of amplification of the target genes and the control *act5C* were approximately the same. All the results were normalized with respect to *act5C*. P-values were measured using one-tailed student's *t* test.

Online supplemental material

Fig. S1 shows that $pcm^{\Delta 1}$ and *ski3* are loss of function alleles. Fig. S2 shows that piRNA production is unaffected in the mRNA degradation mutants. Table S1 shows primer sequences. Online supplemental material is available at http://www.jcb.org/cgi/content/full/jcb.200904063/DC1.

We thank A. Spradling, A. Nakamura, P.M. MacDonald, D. St. Johnson (The Wellcome/CRC Institute, Cambridge, England, UK), T.B. Chou (Institute of Molecular and Cellular Biology, Taipei, Taiwan), S. Newbury (Brighton and Sussex Medical School, Brighton, England, UK), J. Wilhelm, R.M. Long, and the *Drosophila* Stock Center for the fly stocks and antibodies, and especially H. Han for her unpublished anti-AUB. We would also like to thank S. Cohen for critical reading of the manuscript. We are grateful to our laboratory members B. He, J.W. Pek, and V. Patil for their support in the laboratory work and O. Pontes for her advice on small RNA in situ.

A.K. Lim is supported by the Singapore Millennium Foundation program.

Submitted: 13 April 2009
Accepted: 7 July 2009

References

Anderson, P. 2005. A place for RNAi. *Dev. Cell.* 9:311–312.

Aravin, A.A., N.M. Naumova, A.V. Tulin, V.V. Vagin, Y. Rozovsky, and V. Gvozdev. 2001. Double-stranded RNA-mediated silencing of genomic tandem repeats and transposable elements in the *D. melanogaster* germline. *Curr. Biol.* 11:1017–1027.

Aravin, A.A., R. Sachidanandam, A. Girard, K. Fejes-Toth, and G.J. Hannon. 2007. Developmentally regulated piRNA clusters implicate MILI in transposon control. *Science.* 316:744–747.

Barbee, S.A., P.S. Estes, A.M. Cziko, J. Hillebrand, R.A. Luedeman, J.M. Coller, N. Johnson, I.C. Howlett, C. Geng, R. Ueda, et al. 2006. Staufen- and FMRP-containing neuronal RNPs are structurally and functionally related to somatic P-bodies. *Neuron.* 52:997–1009.

Beaudoin, S., B. Vanderperre, C. Grenier, I. Tremblay, F. Leduc, and X. Roucou. 2009. A large ribonucleoprotein particle induced by cytoplasmic PrP shares striking similarities with the chromatoid body, an RNA granule predicted to function in posttranscriptional gene regulation. *Biochim. Biophys. Acta.* 1793:335–345.

Behm-Ansmant, I., J. Rehwinkel, T. Doerks, A. Stark, P. Bork, and E. Izaurralde. 2006. mRNA degradation by miRNAs and GW182 requires both CCR4:NOT deadenylase and DCP1:DCP2 decapping complexes. *Genes Dev.* 20:1885–1898.

Bertrand, E., P. Chartrand, M. Schaefer, S.M. Shenoy, R.H. Singer, and R.M. Long. 1998. Localization of *ash1* mRNA particles in living yeast. *Mol. Cell.* 2:437–445.

Brennecke, J., A.A. Aravin, A. Stark, M. Dus, M. Kellis, R. Sachidanandam, and G.J. Hannon. 2007. Discrete small RNA-generating loci as master regulators of transposon activity in *Drosophila. Cell.* 128:1089–1103.

Buszczak, M., S. Paterno, D. Lighthouse, J. Bachman, J. Planck, S. Owen, A.D. Skora, T.G. Nystul, B. Ohlstein, A. Allen, et al. 2007. The Carnegie protein trap library: a versatile tool for *Drosophila* developmental studies. *Genetics.* 175:1505–1531.

Chambeyron, S., A. Popkova, G. Payen-Groschene, C. Brun, D. Laouini, A. Pelisson, and A. Bucheton. 2008. piRNA-mediated nuclear accumulation of retrotransposon transcripts in the *Drosophila* female germline. *Proc. Natl. Acad. Sci. USA.* 105:14964–14969.

Chen, Y., A. Pane, and T. Schupbach. 2007. *cutoff* and *aubergine* mutations result in retrotransposon upregulation and checkpoint activation in *Drosophila. Curr. Biol.* 17:637–642.

Coller, J.M., M. Tucker, U. Sheth, M.A. Valencia-Sanchez, and R. Parker. 2001. The DEAD box helicase, Dhh1p, functions in mRNA decapping and interacts with both the decapping and deadenylase complexes. *RNA.* 7:1717–1727.

Ding, L., A. Spencer, K. Morita, and M. Han. 2005. The developmental timing regulator AIN-1 interacts with miRISCs and may target the Argonaute protein ALG-1 to cytoplasmic P-bodies in *C. elegans. Mol. Cell.* 19:437–447.

Drummond-Barbosa, D., and A. Spradling. 2004. Alpha-endosulfine, a potential regulator of insulin secretion is required for adult tissue growth control in *Drosophila. Dev. Biol.* 266:310–321.

Eulalio, A., I. Behm-Ansmant, and E. Izaurralde. 2007. P bodies: at the crossroads of post-transcriptional pathways. *Nat. Rev. Mol. Cell Biol.* 8:9–22.

Findley, S.D., M. Tamanaha, N.J. Clegg, and H. Ruohola-Baker. 2003. *Maelstrom*, a *Drosophila* spindle-class gene, encodes a protein that colocalizes with Vasa and RDE1/AGO1 homolog, Aubergine, in nuage. *Development.* 130:859–871.

Forrest, K.M., and E.R. Gavis. 2003. Live imaging of endogeneous RNA reveals a diffusion and entrapment mechanism for *nanos* mRNA localization in *Drosophila. Curr. Biol.* 13:1159–1168.

Gallo, C.M., E. Munro, D. Rasoloson, C. Merritt, and G. Seydoux. 2008. Processing bodies and germ granules are distinct RNA granules that interact in *C. elegans* embryos. *Dev. Biol.* 323:76–87.

Gillespie, D.E., and C.A. Berg. 1995. Homeless is required for RNA Localization in *Drosophila* oogenesis and encodes a new member of the DE-H family of RNA-dependent ATPases. *Genes Dev.* 9:2495–2508.

Gonzalez-Reyes, A., H. Elliott, and D. St Johnston. 1997. Oocyte determination and the origin of polarity in *Drosophila*: the role of spindle genes. *Development.* 124:4927–4937.

Gunawardane, L.S., K. Saito, K.M. Nishida, K. Miyoshi, Y. Kawamura, T. Nagami, H. Siomi, and M.C. Siomi. 2007. A slicer-mediated mechanism for repeat-associated siRNA 5′ end formation in *Drosophila. Science.* 315:1587–1590.

Harris, A.N., and P.M. Macdonald. 2001. Aubergine encodes a *Drosophila* polar granule component required for pole cell formation and is related to eIF2C. *Development.* 128:2823–2832.

Houwing, S., L.M. Kamminga, E. Berezikov, D. Cronembold, A. Girard, H. van den Elst, D.V. Filippov, H. Blaser, E. Raz, C.B. Moens, et al. 2007. A role for Piwi and piRNAs in germ cell maintenance and transposon silencing in zebrafish. *Cell.* 129:69–82.

Jagannath, A., and M.J. Wood. 2009. Localization of double-stranded small interfering RNA to cytoplasmic processing bodies is Ago2 dependent and results in up-regulation of GW182 and Argonaute-2. *Mol. Biol. Cell.* 20:521–529.

Kennerdell, J.R., S. Yamaguchi, and R.W. Carthew. 2002. RNAi is activated during *Drosophila* oocyte maturation in a manner dependent on Aubergine and Spindle-E. *Genes Dev.* 16:1884–1889.

Klenov, M.S., S.A. Lavrov, A.D. Stolyarenko, S.S. Ryazansky, A.A. Aravin, T. Tuschl, and V. Gvozdev. 2007. Repeat-associated siRNAs cause chromatin silencing of retrotransposons in the *Drosophila melanogaster* germline. *Nucleic Acids Res.* 35:5430–5438.

Kotaja, N., S.N. Bhattacharyya, L. Jaskiewicz, S. Kimmins, M. Parvinen, W. Filipowicz, and P. Sassone-Corsi. 2006. The chromatoid body of male germ cells: similarity with processing bodies and presence of Dicer and microRNA pathway components. *Proc. Natl. Acad. Sci. USA.* 103:2647–2652.

Kotelnikov, R.N., M.S. Klenov, Y. Rozovsky, L.V. Olenina, M.V. Kibanov, and V. Gvozdev. 2009. Peculiarities of piRNA-mediated post-transcriptional silencing of *stellate* repeats in testes of *Drosophila melanogaster. Nucleic Acids Res.* 37:3254–3263.

Lall, S., F. Piano, and R.E. Davis. 2005. *Caenorhabditis elegans* decapping proteins: localization and functional analysis of DCP1, DCP2 and DCPS during embryogenesis. *Mol. Biol. Cell.* 16:5880–5890.

Lau, N.C., A.G. Seto, J. Kim, S. Kuramochi-Miyagawa, T. Nakano, D.P. Bartel, and R.E. Kingston. 2006. Characterization of the piRNA complex from rat testes. *Science.* 313:363–367.

Li, C., V.V. Vagin, S. Lee, J. Xu, S. Ma, H. Xi, H. Seitz, M.D. Horwich, M. Syrzycka, B.M. Honda, et al. 2009. Collapse of germline piRNAs in the absence of Argonaute3 reveals somatic piRNAs in flies. *Cell.* 137:509–521.

Lim, A.K., and T. Kai. 2007. A unique germline organelle, Nuage, functions to repress selfish genetic elements in *Drosophila melanogaster. Proc. Natl. Acad. Sci. USA.* 104:6714–6719.

Lin, M.D., S.J. Fan, W.S. Hsu, and T.B. Chou. 2006. *Drosophila* decapping protein 1, dDCP1, is a component of the *oskar* mRNA complex and directs its posterior localization in the oocyte. *Dev. Cell.* 10:601–613.

Lin, M.D., X. Jiao, D.P. Grima, S.F. Newbury, M. Kiledjian, and T.B. Chou. 2008. *Drosophila* processing bodies in oogenesis. *Dev. Biol.* 322:276–288.

Liu, J., F.V. Rivas, J. Wohlschlegel, J.R. Yates III, R. Parker, and G.J. Hannon. 2005a. A role for the P-body component GW182 in microRNA function. *Nat. Cell Biol.* 7:1261–1266.

Liu, J., M.A. Valencia-Sanchez, G.J. Hannon, and R. Parker. 2005b. MicroRNA-dependent localization of targeted mRNAs to mammalian P-bodies. *Nat. Cell Biol.* 7:719–723.

Malone, C.D., J. Brennecke, M. Dus, A. Stark, W.R. McCombie, R. Sachidanandam, and G.J. Hannon. 2009. Specialized piRNA pathways act in germline and somatic tissues of the *Drosophila* ovary. *Cell.* 137:522–535.

Morris, J.Z., A. Hong, M.A. Lilly, and R. Lehmann. 2005. Twin, a CCR4 homolog, regulates cyclin poly(A) tail length to permit *Drosophila* oogenesis. *Development.* 132:1165–1174.

Nishida, K.M., K. Saito, T. Mori, Y. Kawamura, T. Nagami-Okada, S. Inagaki, H. Siomi, and M.C. Siomi. 2007. Gene silencing mechanisms mediated by Aubergine-piRNA complexes in *Drosophila* male gonad. *RNA.* 13:1911–1922.

Orban, T.I., and E. Izaurralde. 2005. Decay of mRNAs targeted by RISC requires XRN1, the Ski complex, and the exosome. *RNA.* 11:459–469.

Pane, A., K. Wehr, and T. Schupbach. 2007. Zucchini and squash encode two putative nucleases required for rasiRNA production in the *Drosophila* germline. *Dev. Cell.* 12:851–862.

Parker, R., and U. Sheth. 2007. P-bodies and the control of mRNA translation and degradation. *Mol. Cell.* 25:635–646.

Pontes, O., C.F. Li, P.C. Nunes, J. Haag, T. Ream, A. Vitins, S.E. Jacobsen, and C.S. Pikaard. 2006. The *Arabidopsis* chromatin-modifying nuclear siRNA pathway involves a nucleolar RNA processing center. *Cell.* 126:79–92.

Salles, F.J., W.G. Richards, and S. Strickland. 1999. Assaying the polyadenylation state of mRNAs. *Methods.* 17:38–45.

Savitsky, M., D. Kwon, P. Georgiev, A. Kalmykova, and V. Gvozdev. 2006. Telomere elongation is under the control of the RNAi-based mechanism in the *Drosophila* germline. *Genes Dev.* 20:345–354.

Schupbach, T., and E. Wieschaus. 1991. Female sterile mutations on the second chromosomes of *Drosophila melanogaster*. II. Mutations blocking oogenesis or altering egg morphology. *Genetics.* 129:1119–1136.

Sen, G.L., and H.M. Blau. 2005. Argonaute 2/RISC resides in sites of mammalian mRNA decay known as cytoplasmic bodies. *Nat. Cell Biol.* 7:633–636.

Shpiz, S., D. Kwon, Y. Rozovsky, and A. Kalmykova. 2009. rasiRNA pathway controls antisense expression of *Drosophila* telomeric retrotransposons in the nucleus. *Nucleic Acids Res.* 37:268–278.

Snee, M.J., and P.M. Macdonald. 2004. Live imaging of nuage and polar granules: evidence against a precursor-product relationship and a novel role for Oskar in stabilization of polar granule components. *J. Cell Sci.* 117:2109–2120.

Till, D.D., B. Linz, J.E. Seago, S.J. Elgar, P.E. Marujo, M. Lourdes Elias, C.M.M. Arraiano, J.A. McClellan, J.E.G. McCarthy, and S.F. Newbury. 1998. Idenfication and developmental expression of a 5′-3′ exoribonuclease from *Drosophila melanogaster. Mech. Dev.* 79:51–55.

Vagin, V.V., A. Sigova, C. Li, H. Seitz, V. Gvozdev, and P.D. Zamore. 2006. A distinct small RNA pathway silences selfish genetic element in the germline. *Science.* 313:320–324.

Van Doren, M., A.L. Williamson, and R. Lehmann. 1998. Regulation of zygotic gene expression in *Drosophila* primordial germ cells. *Curr. Biol.* 8:243–246.

Wilson, J.E., J.E. Connell, and P.M. Macdonald. 1996. Aubergine enhances *oskar* translation in the *Drosophila* ovary. *Development.* 122:1631–1639.

Zabolotskaya, M.V., D.P. Grima, M.D. Lin, T.B. Chou, and S.F. Newbury. 2008. The 5′-3′ exoribonuclease Pacman is required for normal male fertility and is dynamically localized in cytoplasmic particles in *Drosophila* testis cells. *Biochem. J.* 416:327–335.